ACS OMEGA

Article

Cite This: ACS Omega 2019, 4, 11229−11236

http://pubs.acs.org/journal/acsodf

Self-Assembly of Diblock Copolymers Containing Thermo- and Photoresponsive Lower Critical Solution Temperature Phase Behavior Polymer with Tunable Assembly Temperature in an Ionic Liquid Mixture

Xiaoyu Lan,[†] Xiaofeng Ma,[†] Lei Wang,[†] Yijun Shi,[‡] Qun Gu,[§] Linlin Wu,[∥] Xiaoli Gu,*[,⊥] and Zhenyang Luo*[,†]

[†]College of Science and [⊥]College of Chemical Engineering, Nanjing Forestry University, 159 Longpan Road, Nanjing 210037, P. R. China

[‡]Division of Machine Elements, Luleå University of Technology, Luleå 97187, Sweden

[§]Department of Chemistry, Edinboro University of Pennsylvania, 230 Scotland Rd, Edinboro 16444, United States

[∥]College of Materials Science and Engineering, Nanjing Tech University, Nanjing 210009, P. R. China

Supporting Information

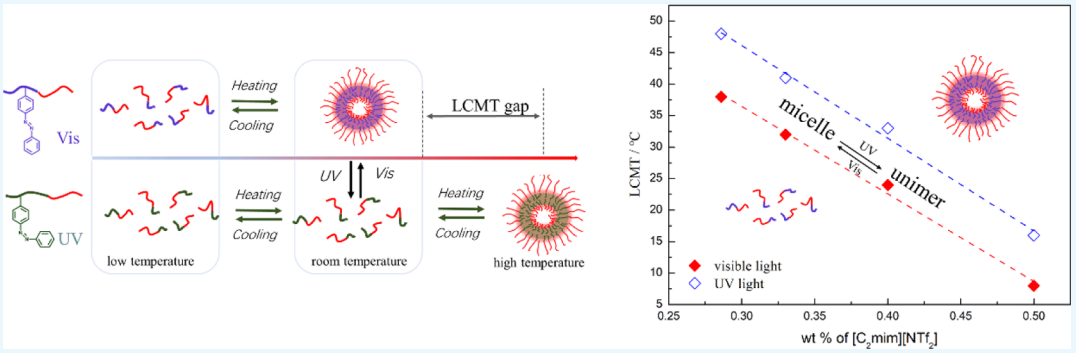

ABSTRACT: This work prepared a type of diblock copolymer with thermo- and photosensitivity in ionic liquids (ILs). P(*N*,*N*-dimethylacrylamide) (compatible with ILs) was prepared as one segment, while butyl acrylate (BA) and 4-phenylazophenylmethacrylate (AzoMA) were copolymerized as another segment P(AzoMA-*r*-BA) with stimuli responsiveness. The diblock copolymer showed tunable lower critical micellization temperature (LCMT) in two mixed imidazole ionic liquids. The value of LCMT depends on not only the conformation status of the azo group in copolymers but also the azo group content in copolymers and mixed ratio of ionic liquids. Based on this tunable LCMT, photoinduced micellization/demicellization can be achieved near room temperature by alternate irradiation with visible and ultraviolet light, and it is totally reversible.

1. INTRODUCTION

Ionic liquid (IL) refers to a liquid composed of ions or ionic pairs, such as KCl or KOH at high temperatures. Among them, room-temperature ILs caused by the loose structure of anion and cation have aroused great concern of scientists because of their physical and chemical properties. The commonality of these properties, such as nonvolatility, wide potential window, nonburning property, and wide electrochemical stability,[1−6] have a wide range of applications starting from their use as green solvents in organic synthesis and a gas separation membrane, to electrodes in batteries, and so on.[7−10] ILs show excellent properties in the fabrication of functional soft materials because of their good compatibility with certain synthetic polymers.[11,12] It was reported that, there is a lower critical solution temperature (LCST) caused by the interaction between poly(benzylmethacrylate) (PBnMA) and a specific IL,[13] which was first demonstrated in pure water by using poly(*N*-isopropylacrylamide) (PNIPAm).[14] In addition, the modified PBnMA would show different properties, for example, the polymer modified by nitration showed no phase behavior in ILs.[15] Now, the polymers like polyacrylate[16] or poly(ethylene oxide)[17,18] are all proved to have ability in presenting the behavior of phase change in ILs with a special performance. When the light-responsive group AzoMA was introduced into a thermoresponsive polymer, the phase separation may be controlled by temperature and light source at the same time.[19]

Received: May 5, 2019
Accepted: June 18, 2019
Published: June 27, 2019

DOI: 10.1021/acsomega.9b01287
ACS Omega 2019, 4, 11229−11236

Scheme 1. Preparation Route for PDMA-*b*-P(AzoMA-*r*-BA) Diblock Copolymer

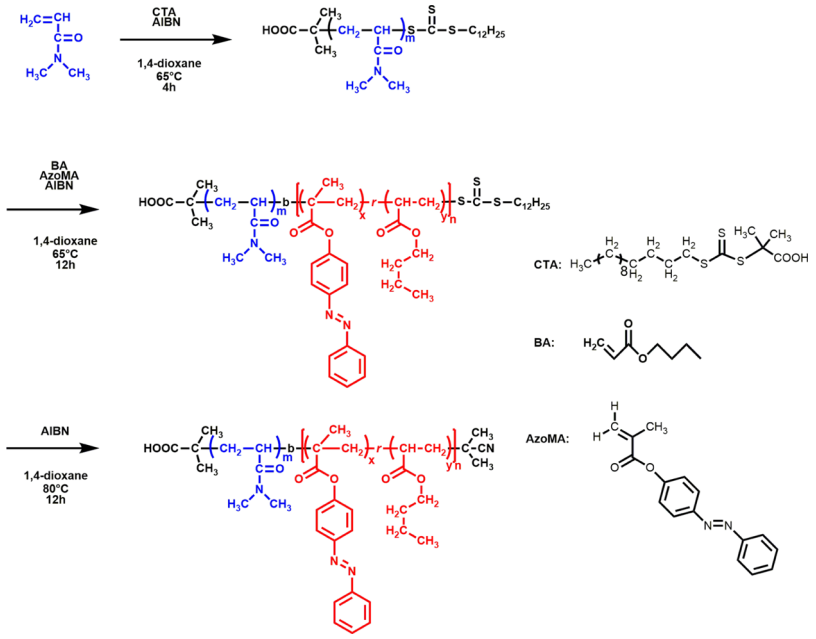

Block copolymers, also known as the mosaic copolymer, is a specific polymer synthesized by joining together two or more polymer segments of different properties. In ILs, they can be self-assembled into different morphologies at low concentration, such as sphere, vesicle, or wormlike micelle, which has been directly observed from cryo-transmission electron microscopy (TEM).[20] In addition, it was reported the thermoresponsive assembly and disassembly of block copolymers contain PNIPAm or PBnMA in ILs, where the PNIPAm showed upper critical solution temperature (UCST).[21,22] Once the azo-containing agents were copolymerized with the UCST-type polymer as one segment in the block copolymer, they would show the behavior of thermo- and photosensitive assembly in ILs.[23,24] These block copolymers showed different upper critical micellization temperature in ILs when the light source was switched between visible light and ultraviolet light. As to the system with lower critical micellization temperature (LCMT) in ILs, very recently, Hall and Lodge reported a photoresponsive block copolymer in concentrated conditions that underwent the reversible order−disorder transition with the action of the AzoMA-PBnMA system and expanded the area of thermo- and photoresponsive materials.[25] Although there are many studies of light-induced micellization based on the PBnMA or PNIPAm in the IL, the temperature for unimer−micelle transition is usually too high, which will restrict their practical use in most cases. Lodge and co-workers found that the LCST of poly(butyl acrylate) can be adjusted to a temperature range from room temperature to more than 200 °C by simply using blends of different imidazole ILs with different lengths of alkyl.[16] According to this, we aimed to realize the photoinduced micellization near room temperature.

Herein, a series of AB-type diblock copolymers consisted of poly(*N*,*N*-dimethylacrylamide) (PDMA: compatible with ILs) as A block and poly(AzoMA-*r*-butyl acrylate) (P(AzoMA-*r*-BA): temperature- and photosensitive polymer in ILs) as B block were synthesized by two-step reversible addition−fragmentation chain transfer (RAFT) copolymerization of AzoMA and butyl acrylate (BA), initiating from the ends of the initiator attached to the PDMA. The PDMA-*b*-P(AzoMA-*r*-BA) copolymers were evidenced to exhibit LCMT transition in ILs mixture, 1-ethyl-3-methylimidazolium bis (trifluoromethane sulfone) imide ($[C_2mim][NTf_2]$) and 1-butyl-3-methylimidazolium bis (trifluoromethanesulfone)imide ($[C_4mim][NTf_2]$) by dynamic light scattering (DLS) measurements. The LCMT of the diblock copolymer can be altered by different photoisomerization states of AzoMA and its value when excited by ultraviolet light was generally higher than that of the block copolymer with stable *trans*-azo. Also, the value of LCMT for PDMA-*b*-P(AzoMA-*r*-BA) can be readily tuned by changing composition of IL mixture. At the intermediate temperature between both LCMTs mentioned above, the self-assembly and disassembly can be controlled by changing the light source. The recoverability of the light-induced micellization was further demonstrated.

2. EXPERIMENTAL SECTION

2.1. Materials. BA, 1,4-dioxane, *N*,*N*-dimethylacrylamide (DMA), diethyl ether, and hexane were purchased from Aladdin. DMA and BA were purified by passing through alumina column. $[C_2mim][NTf_2]$ and $[C_4mim][NTf_2]$ were purchased from Lan Zhou Green Chem. 2-(Dodecylthiocarbonothioylthio)-2-methylpropionic acid (CTA) was prepared by the method in published papers.[26,27] AzoMA was prepared according to the information from the previous study.[28,29] 2,2′-Azobis (isobutyronitrile) (AIBN) was refined by recrystallization from methanol and dried under vacuum before using. The remaining agents were used directly.

2.2. Synthesis of the PDMA-*b*-P(AzoMA-*r*-BA) Diblock Copolymer. Scheme 1 illustrated the typical process of synthesizing the relevant diblock copolymer via RAFT polymerization. A mixture of DMA (6.00 g, 0.060 mol), CTA (0.10 g, 0.30 mmol), and AIBN (9.8 mg, 0.06 mmol) was mixed with the 1,4-dioxane (24.00 g) in a reaction tube filled with the N_2 atmosphere. After the solid agents were totally dissolved in the solvents, the reaction tube was heated at 65 °C for 4 h. Then, the mixture was cooled down to low temperature and dropped into diethyl ether (poor solvent for

DOI: 10.1021/acsomega.9b01287
ACS Omega 2019, 4, 11229−11236

the block copolymer) to precipitate. Using acetone as good solvent, reprecipitations were conducted three times to refine the crude product to obtain the PDMA-CTA (as A block).

Then, P(AzoMA-*r*-BA) (as B block) was polymerized at the end of the PDMA-CTA. Here, PDMA-CTA (1.00 g, 0.08 mol), BA (5.52 g, 0.043 mol), and AzoMA (0.45 g, 1.70 mmol) were first dissolved in a reaction tube filled with inert gas. For the accuracy of weighing, AIBN (0.016 g, 0.10 mmol) was diluted using 10 mL of 1,4-dioxane, then, 1 mL of AIBN solution was extracted and injected to the reaction tube. The reaction was then conducted at 65 °C for 24 h. Similar to the purification of PDMA-CTA, the crude product here was also refined by three times reprecipitation using acetone to redissolve the polymer and hexane to precipitate.

The last step aimed to remove the active trithiocarbonate of each molecular chain. The relevant operation was conducted as follows: the diblock copolymer containing RAFT agent (2.00 g), AIBN (0.42 g) and 1,4-dioxane (50 mL) were directly mixed in a reaction tube filled with inert atmosphere. Then, the reaction tube was heated at 80 °C for 12 h. Apart from the identical purification procedure above, the obtained product was further purified by fractional precipitation. The product precipitated from hexane was mixed with methanol at a concentration of 5%. Then, the mixtures were placed in a low-temperature environment for several days. After filtering out the very little impurities, the product was collected again by precipitating in the hexane. The ultimate products were dried and showed a state of rubbery then.

2.3. Preparation of ILs Mixture Solution Containing Diblock Copolymer. The viscosity of $[C_2mim][NTf_2]$ or $[C_4mim][NTf_2]$ is usually too high and it is difficult for the diblock copolymer to dissolve immediately. Therefore, the IL solution containing the diblock copolymer was prepared using the co-solvent methods. In a small screw bottle, a small amount of tetrahydrofuran (THF) was used to dissolve the diblock copolymer with constant stirring. When the solution was totally clear, a certain composition of $[C_2mim][NTf_2]$ and $[C_4mim][NTf_2]$ was added into the mixture. Then, the THF would be evaporated slowly when the uniform mixture was obtained. It is noted that the 0.22 μm organic filter should be always used to filter the small particles in order to reduce the mistakes that may happen.

2.4. Size Exclusion Chromatography Measurements and ^{1}H NMR Measurements. Size exclusion chromatography (SEC) and ^{1}H NMR measurements are two main means to investigate the structure of the block copolymer. The SEC here was corrected by the universal calibration curve using ten narrowly distributed polystyrene standards. ^{1}H NMR was obtained using Bruker AVANCE III (600 MHz).

2.5. DLS Tests. The particle size and distribution in ILs were investigated by DLS tests. By controlling the temperature with an error no larger than 0.1 °C, the LCMT can be defined from the temperature dependence of size curves. The samples in the quartz cell (to avoid the absorption of ultraviolet light) should be kept for sufficient time to maintain a balanced state once the temperature is tuned slightly. Both visible light (>400 nm, 4 mW/cm^2) and ultraviolet light (365 nm, 8 mW/cm^2) sources are light-emitting diode cold light sources in order to avoid the heat generated by the lamp. It is noted that the particle size determined by DLS refers to the hydrodynamic radius that is calculated from electric field correlation function by relevant equations (Stokes–Einstein equation, method of Cumulants, etc.) whenever in monodisperse solutions or polydisperse solutions.[30]

2.6. UV–Vis Measurements. The photo-reversible transition of the azo group from trans to cis in the diblock copolymer was demonstrated by UV–vis measurements. In order to obtain a spectrum with reasonable absorbance, the contents of the diblock copolymer in ILs was set as 0.13 g/L.

2.7. TEM Measurements. The TEM observation was operated on JEM-1400 at 80 kV. In order to reduce the blocking effect of ILs on electrons, THF was used to dilute the sample to a proper concentration, then, a droplet of dispersion was placed onto a copper grid without the staining agent, and the THF residue was evaporated at 70 °C for an hour before measurements.

3. RESULTS AND DISCUSSION

3.1. Characterization Results of the Diblock Copolymer. The molecular weight of the polymer was determined both by SEC and ^{1}H NMR. The content of AzoMA in diblock copolymers is determined from integrated signal ratio of ^{1}H NMR spectra. Figures 1 and S1 showed a typical ^{1}H NMR and

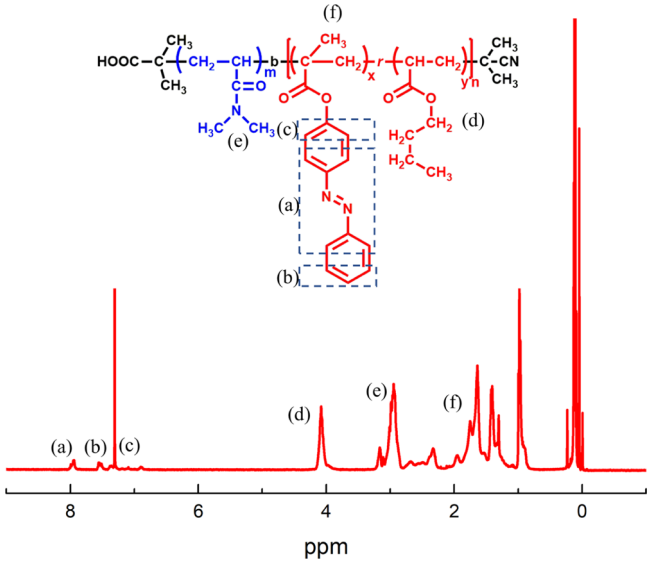

Figure 1. ^{1}H NMR of PDMA-*b*-P(AzoMA$_{13.8}$-*r*-BA) in $CDCl_3$, (a–f) used to mark the attribution of each hydrogen.

SEC traces of the block copolymer, respectively, according to which the characterization results are summarized and shown in Table 1. It is noted that the molecular weight and polydispersity index of homopolymer PDMA were determined by SEC in the first place. Based on the *M*n of PDMA, the *M*n of the block copolymer was determined by comparing the integrated signals from the BA (d) and AzoMA (a) with that of peaks (e) from the DMA in the ^{1}H NMR spectrum. The SEC profiles of polymers were unimodal, however, the dispersity index of PDMA-*b*-P(AzoMA-*r*-BA) in Table 1 was larger than that of PDMA, that is because the azobenzene has the effect of preventing radical polymerization to a certain degree.[31] The content of AzoMA in diblock copolymers was calculated by comparing the integrated signals from AzoMA (a) and signals from the BA (d). In addition, the reagents required for the relevant reaction were characterized by ^{1}H NMR (see Figures S2–S4)

DOI: 10.1021/acsomega.9b01287
ACS Omega 2019, 4, 11229–11236

Table 1. Summary of Data for Diblock Copolymer Obtained by SEC and ^{1}H NMR

polymer	[AzoMA]/[BA] in feed	M_n (kDa)	polydispersity index[a]	[AzoMA]/[BA][b]	polymerization degree	f_{PDMA}[c]
PDMA		11.9[a]	1.06		120	
PDMA-*b*-P(AzoMA$_{5.2}$-*r*-BA)	2/98	31.2[b]	1.15	5.2/94.8	120−142	0.38
PDMA-*b*-P(AzoMA$_{11.0}$-*r*-BA)	4/96	32.1[b]	1.17	11.0/89.0	120−150	0.37
PDMA-*b*-P(AzoMA$_{13.8}$-*r*-BA)	6/94	31.9[b]	1.22	13.8/86.2	120−135	0.37

[a]Characterized by SEC (mobile phase: *N*,*N*-dimethylformamide containing 0.1 mol/L lithium bromide). [b]Calculated from ^{1}H NMR. [c]Calculated form Materials Studio (ρ_{PDMA} = 1.096 $\rho_{P(AzoMA\text{-}r\text{-}BA)}$ = 1.094).

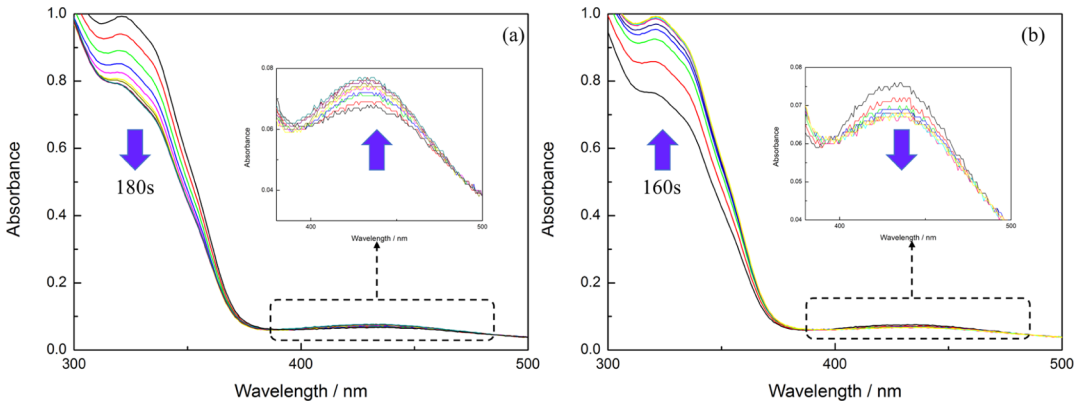

Figure 2. UV−vis spectra of (a) *trans*-to-*cis* photoisomerization of azobenzene in [C$_4$mim][NTf$_2$] when irradiated with ultraviolet light and (b) *cis*-to-*trans* photoisomerization of azobenzene in [C$_4$mim][NTf$_2$] when irradiated with visible light.

As Figure 2 shows, there are two distinct peaks located at 320 and 430 nm, respectively. One peak is caused by the $\pi-\pi^*$ transition of outer electron from *trans*-AzoMA, the other is caused by the n−π^* transition of outer electron from *cis*-AzoMA. Under UV irradiation, the absorption at 320 nm showed an obvious decrease, and the absorption at 430 nm coming from the n−π^* transition of *cis*-AzoMA continued to increase at the same time, indicating AzoMA had undergone the *trans* to *cis* isomerization change. This process took almost 180 s to reach the steady state. After visible light irradiation, the peaks around 320 nm showed a distinct increase, suggesting *cis*-AzoMA had recovered to *trans*-AzoMA. In the meantime, the absorption at 430 nm recovered to the initial state too, and it took almost 160 s to complete this transition. It is obvious that the photoisomerization reaction of PDMA-*b*-P(AzoMA-*r*-BA) in ILs is reversible.

3.2. DLS Characterization and TEM Imaging of the Micelle. Critical micelle concentration (cmc) was determined by DLS measurement of a series of different concentration of solutions of PDMA-*b*-P(AzoMA$_{13.8}$-*r*-BA) in [C$_2$mim][NTf$_2$] (Figure S5). It was found that the cmc was 0.2 wt %. Therefore, the sample of 1 wt % solution of the diblock copolymer in IL was chosen as an example to conduct the following characterization. Figure 3 shows the correlation functions for 1 wt % solutions of PDMA-*b*-P(AzoMA$_{13.8}$-*r*-BA) in ILs mixture ([C$_2$mim][NTf$_2$]/[C$_4$mim][NTf$_2$] = 1/2.5 by weight) with different temperatures. Hydrodynamic radius (R_h) and dispersity index of the particles were obtained from Figure 3 according to the intrinsic equation and shown in Table 2, in which there are two different R_hs when the temperature is below 38 °C. The smaller R_h peak (<10 nm) indicates the hydrodynamic radius of molecular chain itself with molecular weight near 32 kDa, and the peak over 100 nm shows that there are some aggregates that cannot be ignored. The higher dispersity index (>0.2) of particles at low temperatures also indicates the coexistence of smaller particles and larger particles. Figure S6a,b show the intensity distribution and volume distribution of PDMA-*b*-P-

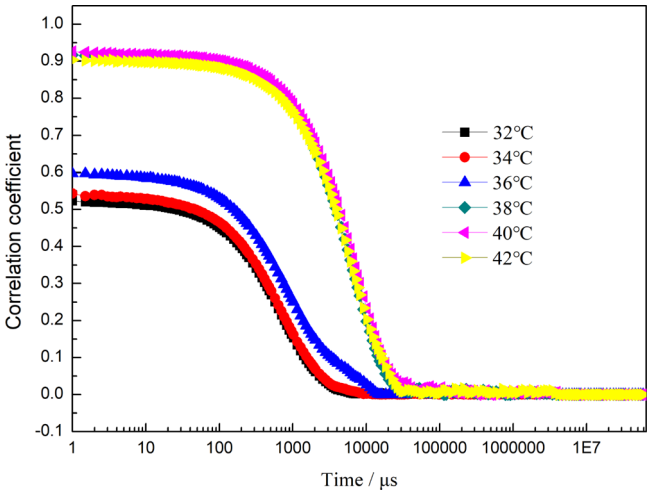

Figure 3. Correlation coefficient for 1 wt % solutions of PDMA-*b*-P(AzoMA$_{13.8}$-*r*-BA) in ILs mixture ([C$_2$mim][NTf$_2$]/[C$_4$mim][NTf$_2$] = 1/2.5 by weight) with different temperatures.

Table 2. Temperature Dependence of R_h and Dispersity Index of 1 wt % Solutions of PDMA-*b*-P(AzoMA$_{13.8}$-*r*-BA) in ILs Mixture ([C$_2$mim][NTf$_2$]/[C$_4$mim][NTf$_2$] = 1/2.5 by Weight)

temperature (°C)	peak 1 R_h (nm)	peak 2 R_h (nm)	dispersity index
32	8.7	106.3	0.275
34	9.6	114.6	0.349
36	8.8	136.4	0.623
38		171.8	0.027
40		182.5	0.031
42		199.6	0.013

DOI: 10.1021/acsomega.9b01287
ACS Omega 2019, 4, 11229−11236

(AzoMA$_{13.8}$-*r*-BA) in ILs mixture ([C_2mim][NTf_2]/[C_4mim][NTf_2] = 1/2.5 by weight) at 32 °C, respectively. The intensity distribution function was bimodal, however, volume distribution function was unimodal, suggesting an amount of the unimers are dominated. The formation of these aggregates is mainly caused by two reasons. The first is possibly the irregular composition of comonomers caused by the random copolymerization, and the second may be the that there are small amounts of macromolecules with very high molecular weight owing to the nonliving polymerization. When the temperature was increased to 36 °C, the phenomenon of coexistence of smaller particles and larger particles still existed. However, both the intensity distribution function and volume distribution function were bimodal (Figure S7), demonstrating parts of unimers had aggregated into micelles.

When the temperatures were elevated above 38 °C, only one R_h of the particles is shown in Table 2, there was only one peak larger than 160 nm and the peak corresponding to the molecular chain was completely gone in both intensity distribution and volume distribution of PDMA-*b*-P(AzoMA$_{13.8}$-*r*-BA) in ILs mixture ([C_2mim][NTf_2]/[C_4mim][NTf_2] = 1/2.5 by weight) at 42 °C (Figure S8a,b). This indicated that unimers had aggregated into micelles. The lower dispersity index (<0.032) of micelles at high temperatures also demonstrated the formation of micelles. The R_hs of the micelles at higher temperatures are >160 nm, suggesting possible formation of a bilayer vesicle or worm-like micelle. In this paper, formation of the bilayer vesicle was proved by TEM images of a 1 wt % solutions of PDMA-*b*-P(AzoMA$_{13.8}$-*r*-BA) in [C_2mim][NTf_2] (because LCMT of 1 wt % solutions of PDMA-*b*-P(AzoMA$_{13.8}$-*r*-BA) in [C_2mim][NTf_2] is lower than room temperature, 1 wt % solutions of PDMA-*b*-P(AzoMA$_{13.8}$-*r*-BA) in the [C_2mim][NTf_2] system was selected to conduct TEM) in Figure 4.

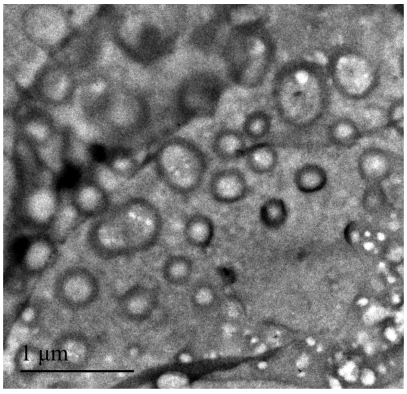

Figure 4. TEM image of PDMA-*b*-P(AzoMA$_{13.8}$-*r*-BA) in [C_2mim][NTf_2].

3.3. Thermoresponsive Micellization/Demicellization of PDMA-*b*-P(AzoMA-*r*-BA) in an IL under Visible and UV Irradiation. The thermoresponsive micellization of the diblock copolymer in single IL [C_4mim][NTf_2] was observed by DLS. Figure 5 showed the particle size of 1 wt % diblock copolymer solution in [C_4mim][NTf_2] with the increasing of temperature under visible or ultraviolet light illumination. At low temperature below the LCMT, the particle size in [C_4mim][NTf_2] was below 10 nm, corresponding to the hydrodynamic radius of the polymer chain itself. As the temperature increased above the LCMT, the smaller particles completely disappeared, and larger particles around 160 nm were formed, indicating formation of micelles (Figure 5a). It is obviously seen that the diblock copolymer containing higher azo contents often has a lower value of LCMT, which is due to the solvophobic nature of PAzoMA, for example, LCMTs for PDMA-*b*-P(AzoMA$_{5.2}$-*r*-BA), PDMA-*b*-P(AzoMA$_{11.0}$-*r*-BA), and PDMA-*b*-P(AzoMA$_{13.8}$-*r*-BA) in [C_4mim][NTf_2] were 103, 93 and 86 °C, respectively (Figure 5b–d), it was getting smaller when the contents of AzoMA were increased. At the same time, under UV irradiation, LCMTs for three polymers were 107, 100, and 94 °C, respectively (Figure 5b–d), the LCMT gap between the UV or visible light irradiation would gradually become smaller when the contents of the azo group were decreased. The LCST phase separation here comes from the cation–π interaction between the polymer and the ILs, according to which the structure solvation lead to the change of entropy. It was well known that the polarity of *cis*-azobenzene excited by ultraviolet light is significantly higher than its *trans*-form.[32] The polymer containing more *cis*-azobenzene would show a better compatibility with ILs, which accounts for the higher LCST of theP(*cis*-AzoMA-*r*-BA) segment, leading to a larger LCMT of PDMA-*b*-P(*cis*-AzoMA-*r*-BA) in ILs ultimately. Additionally, the cation–π interaction between the azo groups is significantly larger than that of BA, making contents of AzoMA play an important role in tuning the LCMT gap.

3.4. Thermo- and PhotoInduced Micellization/Demicellization with Tunable LCMT in Mixed IL. Using single IL [C_4mim][NTf_2] often makes the LCMT larger than 80 °C while the value of LCMT would be lower than 0 °C if the single [C_2mim][NTf_2] is used. To tune the LCMT in a reasonable range, we prepared the solvents with two IL blends. Here, we took PDMA-*b*-P(AzoMA$_{13.8}$-*r*-BA) as an example to investigate the micellization behavior in the [C_2mim][NTf_2]/[C_4mim][NTf_2] mixture under ultraviolet or visible light. As Figure 6 showed, both curves under UV or visible light irradiation showed the transition of unimers to micelles when the temperature was elevated. The LCMTs of PDMA-*b*-P(AzoMA$_{13.8}$-*r*-BA) in ILs mixture ([C_2mim][NTf_2]/[C_4mim][NTf_2] = 1/1.5) for *trans*-form and *cis*-form were 26 and 34 °C, respectively. There was 8 °C difference in the LCMTs between the polymers with different conformation of azobenzene. With the increase of [C_4mim][NTf_2] content in ILs mixture, LCMT under ultraviolet or visible light irradiation increased at the same time.

We can also see that the different composition of ILs would not make the LCMT differences fluctuate greatly when the system was exposed under ultraviolet or visible light, that is because the two ILs has similar polarities and interaction between azo group and [C_2mim][NTf_2] is similar with that of interaction between azo group and [C_4mim][NTf_2].

To further demonstrate the photoinduced micellization of the diblock copolymer in ILs mixture, PDMA-*b*-P(AzoMA$_{13.8}$-*r*-BA) in certain composition of ILs was set at a bistable temperature (28 °C) associated with the change of the light source. As shown, the size of the aggregates in ILs mixture was larger than 100 nm (Figure 7a), which indicated the formation of micelles. When the present system was irradiated with UV light, the size fell to about 8 nm (Figure 7b), indicating that the photoinduced demicellization was successfully realized, as the LCMT of the PDMA-*b*-P(*cis*-AzoMA$_{13.8}$-*r*-BA) is higher than that of PDMA-*b*-P(*trans*-AzoMA$_{13.8}$-*r*-BA). Then, the visible light was switched back again, as expected, the unimers

DOI: 10.1021/acsomega.9b01287
ACS Omega 2019, 4, 11229–11236

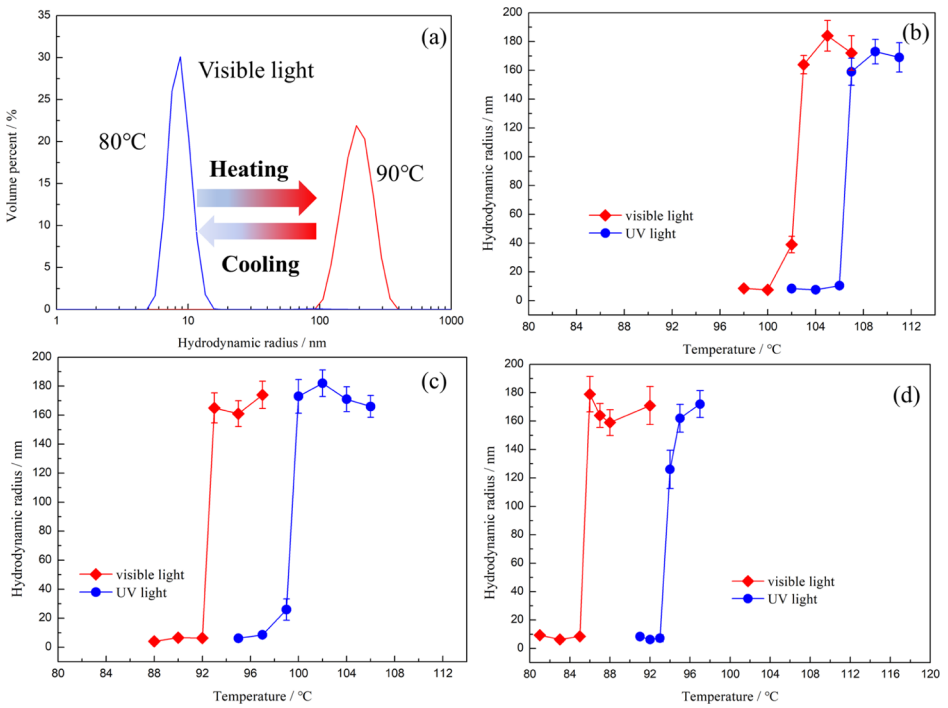

Figure 5. Temperature dependence of size for (a) a representative size change of PDMA-*b*-P(AzoMA$_{13.8}$-*r*-BA) in [C$_4$mim][NTf$_2$] base on DLS measurements; (b) PDMA-*b*-P(AzoMA$_{5.2}$-*r*-BA), (c) PDMA-*b*-P(AzoMA$_{11.0}$-*r*-BA) and (d) PDMA-*b*-P(AzoMA$_{13.8}$-*r*-BA) in [C$_4$mim][NTf$_2$] under UV or visible light.

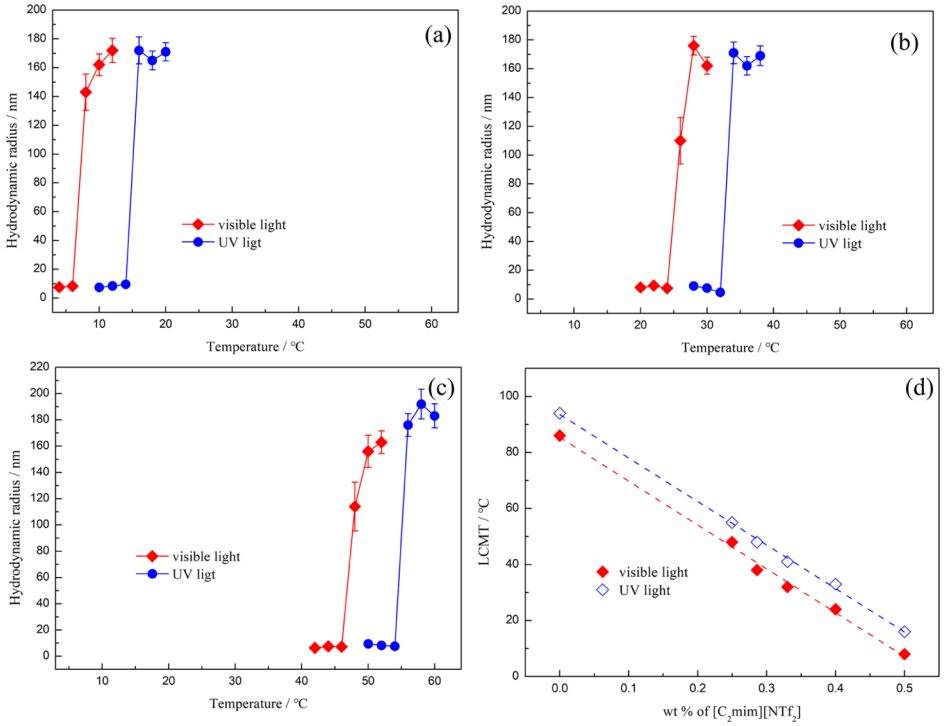

Figure 6. Temperature dependence of size for PDMA-*b*-P(AzoMA$_{13.8}$-*r*-BA) under visible (red line) or UV (blue line) conditions in ILs mixture (a) [C$_2$mim][NTf$_2$]/[C$_4$mim][NTf$_2$] = 1/1 by weight; (b) [C$_2$mim][NTf$_2$]/[C$_4$mim][NTf$_2$] = 1/1.5 by weight; (c) [C$_2$mim][NTf$_2$]/[C$_4$mim][NTf$_2$] = 1/3 by weight; (d) relationship among the temperature, LCMT and composition of ILs.

aggregated into micelles again with the appearance of large size particles (Figure 7c). Insets in Figure 7a−c are sample pictures under corresponding conditions. The sample solution in Figure 7b has a lack of turbidity compared with that in Figure 7a,c, which further confirm the photoinduced unimer micelle transition. Figure 7d illustrates the time dependence of size for the diblock copolymer in IL mixture at 28 °C. It is obvious that there is an induction time for the process of micellization or demicellization. There are two reasons for this induction time; one is that the conformational change of the azobenzene

DOI: 10.1021/acsomega.9b01287
ACS Omega 2019, 4, 11229−11236

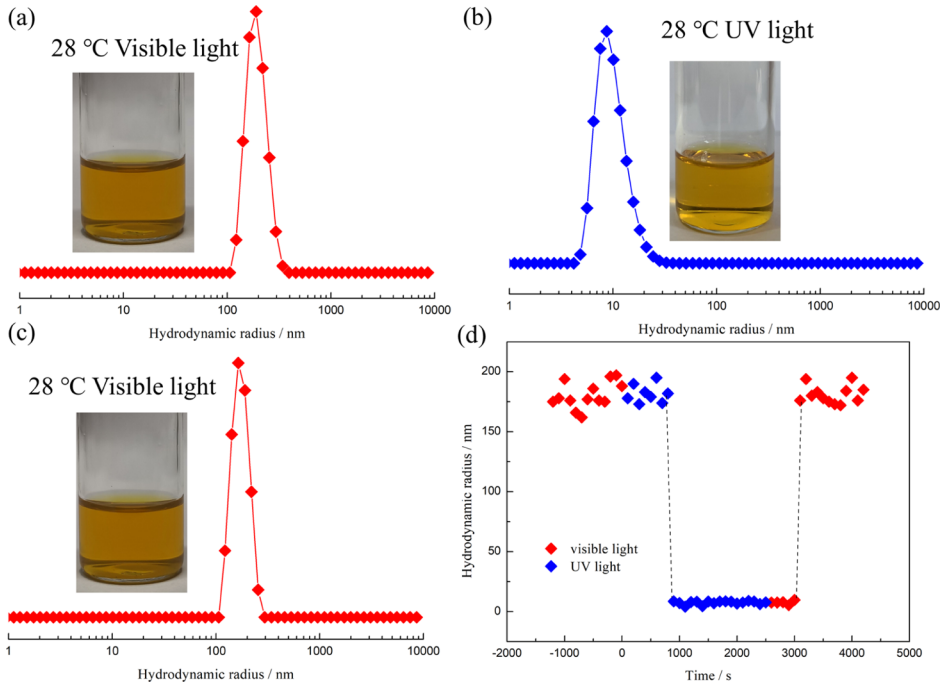

Figure 7. Volume percent of PDMA-*b*-P(AzoMA$_{13.8}$-*r*-BA) in ILs mixture ([C_2mim][NTf_2]/[C_4mim][NTf_2] = 1/1.5 by weight) at 28 °C: (a) irradiated with visible light (b) irradiated with ultraviolet light (c) switched to visible light again; (d) time dependence of size with a different light source.

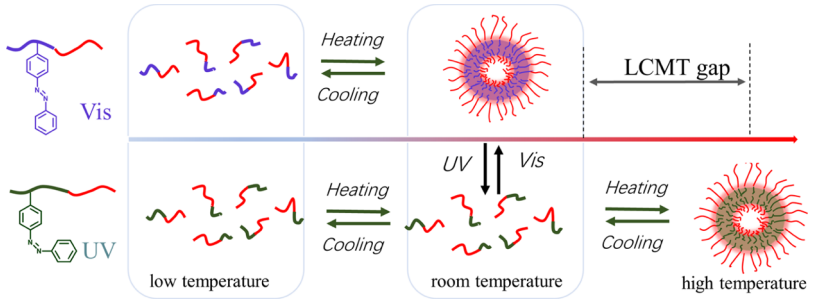

Figure 8. Schematic illustration of the photoinduced micellization near room temperature.

group needs time to be realized, which has been investigated by UV−vis. Another reason is that the diffusions of polymers in ILs are needed for either micellization or demicellization, as multiple polymer chains need time to aggregate together or redissolve in the ILs by overcoming the intermolecular force. From the data given above, we can simply see that the reversible photoinduced micellization can be fully realized by switching the light source.

Here, the reversible light-induced micellization was realized by using the LCMT gap caused by a different light source. The polymer with more contents of *cis*-azobenzene under ultraviolet showed a higher value of LCMT. At an intermediate temperature between the LCMT gap, photoinduced unimer micelle transition was realized, as Figure 8 showed.

4. CONCLUSIONS

In this paper, a type of AB block copolymer was prepared successfully. The PDMA is a segment that can always dissolve in the ILs while the segment of P(AzoMA-BA) presented light and thermoresponsive LCST characteristics in ILs, according to which the thermo- and photoresponsive assemblies in ILs were realized. The LCMT value would be affected by several factors at the same time, such as the contents and the conformation of AzoMA, the different composition of ILs. According to these behaviors, the value of LCMT can be readily tuned to near-room temperature without changing the polymer structure, which will be useful to design a smart room temperature material. Lastly, photoinduced "contactless" reversible unimer micelle transition of block copolymers was realized by using the LCMT gap caused by the different conformation of the azo group. Based on the desirable properties mentioned above, we are hoping to prepare a room temperature artificial actuator in IL based on the LCST of P(AzoMA-*r*-BA).

■ ASSOCIATED CONTENT

Supporting Information

The Supporting Information is available free of charge on the ACS Publications website at DOI: 10.1021/acsomega.9b01287.

^{1}H NMR of products of each step, DLS measurements, and SEC traces of polymers (PDF)

DOI: 10.1021/acsomega.9b01287
ACS Omega 2019, 4, 11229−11236

AUTHOR INFORMATION

Corresponding Authors

*E-mail: guxiaoli@njfu.edu.cn (X.G.).
*E-mail: luozhenyang@njfu.edu.cn (Z.L.).

ORCID

Xiaoli Gu: 0000-0001-8588-0358

Author Contributions

X.L. and X.M. equally contributed to this paper. All authors discussed the results and contributed to the final manuscript.

Funding

This work was supported by the Natural Science Foundation of Jiangsu Province (BK20160992), the Natural Science Foundation of the Jiangsu Higher Education Institutions (15KJB430018), the National Natural Science Foundation of China (no. 21774059), A Project Funded by the Priority Academic Program Development of Jiangsu Higher Education Institutions (PAPD).

Notes

The authors declare no competing financial interest.

ACKNOWLEDGMENTS

The author thanks to the nuclear magnetic resonance provided by Dr. Shilong Yang from the Analytical Testing Center of Nanjing Forestry University. Liwen Mu from Luleå University of Technology is acknowledged for the constructive discussions.

REFERENCES

(1) Wang, B.; Qin, L.; Mu, T.; Xue, Z.; Gao, G. Are ionic liquids chemically stable? *Chem. Rev.* **2017**, *117*, 7113−7131.
(2) Angell, C. A.; Ansari, Y.; Zhao, Z. Ionic liquids: past, present and future. *Faraday Discuss* **2012**, *154*, 9−27.
(3) Hayes, R.; Warr, G. G.; Atkin, R. Structure and nanostructure in ionic liquids. *Chem. Rev.* **2015**, *115*, 6357−6426.
(4) Ueno, K.; Tokuda, H.; Watanabe, M. Ionicity in ionic liquids: correlation with ionic structure and physicochemical properties. *Phys. Chem. Chem. Phys.* **2010**, *12*, 1649−1658.
(5) Xue, Z.; Qin, L.; Jiang, J.; Mu, T.; Gao, G. Thermal, electrochemical and radiolytic stabilities of ionic liquids. *Phys. Chem. Chem. Phys.* **2018**, *20*, 8382−8402.
(6) Yang, Q.; Zhang, Z.; Sun, X.-G.; Hu, Y.-S.; Xing, H.; Dai, S. Ionic liquids and derived materials for lithium and sodium batteries. *Chem. Soc. Rev.* **2018**, *47*, 2020−2064.
(7) Clarke, C. J.; Tu, W.-C.; Levers, O.; Bröhl, A.; Hallett, J. P. Green and sustainable solvents in chemical processes. *Chem. Rev.* **2018**, *118*, 747−800.
(8) Zulfiqar, S.; Sarwar, M. I.; Mecerreyes, D. Polymeric ionic liquids for CO2 capture and separation: potential, progress and challenges. *Polym. Chem.* **2015**, *6*, 6435−6451.
(9) Tomé, L. C.; Marrucho, I. M. Ionic liquid-based materials: A platform to design engineered CO2 separation membranes. *Chem. Soc. Rev.* **2016**, *45*, 2785−2824.
(10) Xu, W.; Ledin, P. A.; Shevchenko, V. V.; Tsukruk, V. V. Architecture, Assembly, and Emerging Applications of Branched Functional Polyelectrolytes and Poly(ionic liquid)s. *ACS Appl. Mater. Interfaces* **2015**, *7*, 12570−12596.
(11) Ueki, T.; Watanabe, M. Macromolecules in ionic liquids: progress, challenges, and opportunities. *Macromolecules* **2008**, *41*, 3739−3749.
(12) Ueki, T.; Watanabe, M. Polymers in Ionic Liquids: Dawn of Neoteric Solvents and Innovative Materials. *Bull. Chem. Soc. Jpn.* **2012**, *85*, 33−50.
(13) Ueki, T.; Watanabe, M. Lower critical solution temperature behavior of linear polymers in ionic liquids and the corresponding volume phase transition of polymer gels. *Langmuir* **2007**, *23*, 988−990.
(14) Heskins, M.; Guillet, J. E. Solution properties of poly (N-isopropylacrylamide). *J. Macromol. Sci., Chem.* **1968**, *2*, 1441−1455.
(15) Kodama, K.; Nanashima, H.; Ueki, T.; Kokubo, H.; Watanabe, M. Lower critical solution temperature phase behavior of linear polymers in imidazolium-based ionic liquids: effects of structural modifications. *Langmuir* **2009**, *25*, 3820−3824.
(16) Lee, H. N.; Lodge, T. P. Poly(n-butyl methacrylate) in Ionic Liquids with Tunable Lower Critical Solution Temperatures (LCST). *J Phys Chem B* **2011**, *115*, 1971−1977.
(17) Kodama, K.; Tsuda, R.; Niitsuma, K.; Tamura, T.; Ueki, T.; Kokubo, H.; Watanabe, M. Structural effects of polyethers and ionic liquids in their binary mixtures on lower critical solution temperature liquid-liquid phase separation. *Polym. J.* **2011**, *43*, 242−248.
(18) Lee, H.-N.; Newell, N.; Bai, Z.; Lodge, T. P. Unusual lower critical solution temperature phase behavior of poly (ethylene oxide) in ionic liquids. *Macromolecules* **2012**, *45*, 3627−3633.
(19) Ueki, T.; Yamaguchi, A.; Ito, N.; Kodama, K.; Sakamoto, J.; Uneo, K.; Kokubo, H.; Watanabe, M. Photoisomerization-induced tunable LCST phase separation of azobenzene-containing polymers in an ionic liquid. *Langmuir* **2009**, *25*, 8845−8848.
(20) He, Y.; Li, Z.; Simone, P.; Lodge, T. P. Self-assembly of block copolymer micelles in an ionic liquid. *J Am Chem Soc* **2006**, *128*, 2745−2750.
(21) Ueki, T.; Watanabe, M.; Lodge, T. P. Doubly thermosensitive self-assembly of diblock copolymers in ionic liquids. *Macromolecules* **2009**, *42*, 1315−1320.
(22) Kobayashi, Y.; Kitazawa, Y.; Komori, T.; Ueno, K.; Kokubo, H. Self-Assembly of Polyether Diblock Copolymers in Water and Ionic Liquids. *Macromol. Rapid Commun.* **2016**, *37*, 1207−1211.
(23) Watanabe, X.; Usui, R.; Kitazawa, Y.; Kokubo, H. Temperature and light-induced self-assembly changes of a tetra-arm diblock copolymer in an ionic liquid. *Polym. J.* **2015**, *47*, 739−746.
(24) Watanabe, T.; Nakamura, Y.; Lodge, T. P.; Watanabe, M. Light-controlled reversible micellization of a diblock copolymer in an ionic liquid. *Macromolecules* **2012**, *45*, 7566−7573.
(25) Hall, C. C.; Lodge, T. P. Photoreversible Order-Disorder Transition in an Ionic LiquidSolvated Block Polymer. *ACS Macro Lett.* **2019**, *8*, 393−398.
(26) Rzayev, J.; Hillmyer, M. A. Nanochannel array plastics with tailored surface chemistry. *J. Am. Chem. Soc.* **2005**, *127*, 13373−13379.
(27) Gooch, A.; Murphy, N. S.; Thomson, N. H.; Wilson, A. J. Side-chain supramolecular polymers employing conformer independent triple hydrogen bonding arrays. *Macromolecules* **2013**, *46*, 9634−9641.
(28) Wu, S.; Zhu, X.; Yang, J.; Nie, J. A facile photopolymerization method for fabrication of pH and light dual reversible stimuli-responsive surfaces. *Chem. Commun.* **2015**, *51*, 5649−5651.
(29) Ye, Q.; Huo, M.; Zeng, M.; Liu, L.; Peng, L.; Wang, X.; Yuan, J. Photoinduced reversible worm-to-vesicle transformation of azo-containing block copolymer assemblies prepared by polymerization-induced self-assembly. *Macromolecules* **2018**, *51*, 3308−3314.
(30) Wang, C.; Hashimoto, K.; Zhang, J.; Kobayashi, Y.; Kokubo, H.; Watanabe, M. Micellization/Demicellization self-Assembly change of ABA triblock copolymers induced by a photoswitchable ionic liquid with a small molecular trigger. *Macromolecules* **2017**, *50*, 5377−5384.
(31) Luo, C.; Zuo, F.; Ding, X.; Zheng, Z.; Cheng, X.; Peng, Y. Light-triggered reversible solubility of a-cyclodextrin and azobenzene moiety complexes in PDMAA-co-PAPA via molecular recognition. *J. Appl. Polym. Sci.* **2008**, *107*, 2118−2125.
(32) Kumar, G. S.; Neckers, D. C. Photochemistry of azobenzene-containing polymers. *Chem. Rev.* **1989**, *89*, 1915−1925.

DOI: 10.1021/acsomega.9b01287
ACS Omega 2019, 4, 11229−11236